

Comparative *ab initio* pseudopotential studies of (2×1) group V overlayers on Si(001)

This article has been downloaded from IOPscience. Please scroll down to see the full text article.

1998 J. Phys.: Condens. Matter 10 7751

(<http://iopscience.iop.org/0953-8984/10/35/009>)

View [the table of contents for this issue](#), or go to the [journal homepage](#) for more

Download details:

IP Address: 171.66.16.209

The article was downloaded on 14/05/2010 at 16:42

Please note that [terms and conditions apply](#).

Comparative *ab initio* pseudopotential studies of (2×1) group V overlayers on Si(001)

S C A Gay, S J Jenkins[†] and G P Srivastava

Physics Department, University of Exeter, Stocker Road, Exeter EX4 4QL, UK

Received 26 February 1998, in final form 9 June 1998

Abstract. We present a comparative theoretical study of a single-monolayer coverage of the group V elements P, As, Sb and Bi on the Si(001) surface. The generic (2×1) surface reconstruction, due to formation of symmetric overlayer dimers, is considered and a first-principles pseudopotential method is used. In addition to presenting well-relaxed structural data, we identify chemical trends in geometry, bonding and electronic structure in moving down the group V column of the periodic table. Overlayer-induced distortion of the substrate is found to decrease with increasing overlayer atomic number. In general, P and As overlayer systems share many similarities, while Sb and Bi form another such natural pair. A novel feature of group V overlayers is that the bonding and occupied antibonding states formed by the dangling bonds lie very close in energy.

1. Introduction

Silicon is already the most studied of all semiconducting materials and yet remains a rich source of new inspiration as a result of its varied properties and central technological role. The nature of clean and covered Si surfaces has lately been of particular interest, with increased miniaturization of devices ensuring that surface effects may no longer safely be ignored. Of the various surfaces now artificially grown by the molecular beam epitaxy (MBE) method, the (001) surface is the most common and technologically vital. At very low temperatures the Si(001) surface adopts a $c\text{--}(2 \times 4)$ reconstruction [1, 2] featuring alternately buckled Si dimers. At higher temperatures, this changes to an apparent (1×2) reconstruction [3–5] due to the rapid thermal flipping of these dimers. At the lowest level, the essential building block for the reconstruction of the Si(001) clean surface is thus the single buckled dimer.

The behaviour of group V elements on Si(001) surfaces is of potential technological importance and is scientifically interesting. It is well known that As [6, 7], Sb [7, 8] and Bi [8] act as surfactants for the epitaxial growth of Ge on the Si(001) surface. Termination of the Si(001) surface with As is also of interest as a first stage in the epitaxial growth of GaAs on Si [9]. In addition P, As and Sb are important dopants, so an understanding of their interaction with the Si substrate would be helpful.

This study compares the various properties of a monolayer (1ML) deposition of four group V elements, namely P, As, Sb and Bi, on the Si(001) surface. Overlayers of As [10, 11] and Sb [12] cause a (2×1) reconstruction on the Si(001) surface, characterized

[†] Present address: Department of Chemistry, University of Cambridge, Lensfield Road, Cambridge CB2 1EW, UK.

by the breaking of the Si dimers and the formation of adsorbate dimers perpendicular to the original Si dimers of the (1×2) substrate. No experimental data are yet available for the Si(001)/P(1ML) surface. However, we have used the (2×1) reconstruction for the purposes of this comparative study.

In contrast, LEED experiments reveal that the larger Bi atoms form a $(2 \times n)$ reconstruction on the Si(001) substrate, with n ranging from 13 at temperatures around 400 K down to 5 at temperatures of 800 K and above [13, 14]. However, the basic building block of the $(2 \times n)$ structure is again the single Bi dimer: the unit cell contains $(n - 1)$ Bi dimers, with space for one missing Bi dimer. Recognizing this fact, and in the interests of comparison, we chose to study (2×1) reconstructions for all four overlayers considered, including Bi.

In particular, in this paper, we compare the nature of the different overlayer dimers themselves, addressing such matters as their symmetry, bonding (both within the dimer and between dimer and substrate) and whether they give rise to surface states inside the fundamental band gap. We also comment on patterns of substrate relaxation in the presence of the overlayer. We have discussed certain aspects of the Sb and Bi overlayer systems separately in previous publications [15–17], but the inclusion of P and As overlayers in the present work allows us to identify important chemical trends in descending group V of the periodic table.

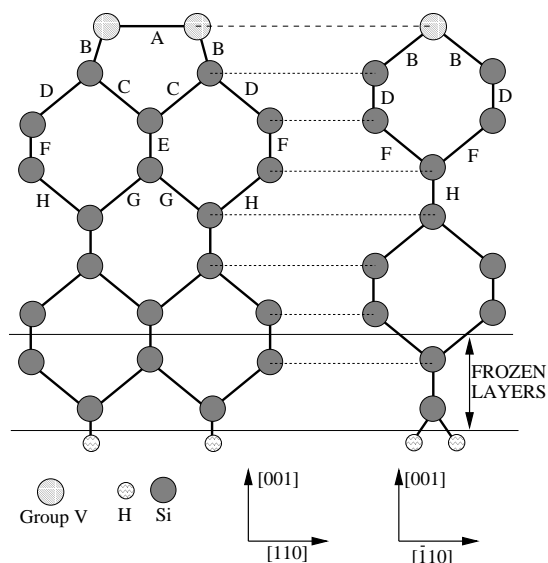


Figure 1. A schematic diagram showing the geometry of the Si(001)/V- (2×1) unit cell used in all of the calculations. Various bonds are labelled A–H and are referenced as such in the text, figures and tables.

2. Method

The *ab initio* results presented in this paper were obtained using the density functional theory of Hohenberg, Kohn and Sham within the local density approximation [18, 19]. Electron correlation was taken into account using the Ceperley and Alder correlation scheme, as parametrized by Perdew and Zunger [20]. The electron–ion interaction was considered in the form of the norm-conserving pseudopotentials listed by Bachelet, Hamann and Schlüter [21], and a plane-wave basis was used in expanding the wavefunctions. Self-consistent solutions to the Kohn–Sham equations were obtained by using four special k -

points within the irreducible segment of the surface Brillouin zone.

All four sets of calculations were performed using the same size supercell. We considered a (2×1) surface unit cell and introduced an artificial periodicity in the surface-normal direction by using a supercell of length equivalent to 12 atomic layers of bulk Si (at our theoretical bulk Si lattice parameter of 5.42 Å). Each supercell contained a slab of eight atomic layers of Si capped on one side with a monolayer of a group V element. On the opposite side of the slab, the two backmost Si layers were frozen into their bulk positions, and the back surface was passivated with H in a dihydride structure (see figure 1). All atoms other than the back two Si layers were allowed to relax into their minimum-energy positions using a conjugate-gradient method [22].

The surface geometries and band structures were obtained using an 8 Ryd kinetic energy cut-off for the plane-wave basis. Convergence tests up to 12 Ryd for bulk Si demonstrate that this is entirely sufficient to obtain well-converged structural information. The bulk Si bond length is calculated as 2.346 Å, 2.347 Å and 2.342 Å for energy cut-offs at 8 Ryd, 11 Ryd and 12 Ryd respectively. Tests on the Bi overlayer system showed only 0.3% change in the dimer length in going from 8 Ryd up to 10 Ryd. On the other hand band structures obtained at 8 Ryd are *not* fully converged with respect to the cut-off. Nevertheless, they *do* contain all of the *qualitative* features of a fully converged high-cut-off band structure.

Table 1. Dimer bond lengths (in Å) for (2×1) group V overlayers on Si (001). The Pauling radius for the dimer bond is taken as the single covalent normal radius.

		P	As	Sb	Bi
Theory	LDA (this work)	2.28	2.51	2.96	3.06
	LDA [31]	—	—	2.94	—
	LDA [26]	—	2.57	2.94	—
	LDA [30]	—	—	2.96	—
	LDA [25]	—	2.55	—	—
	LDA [24]	—	2.52	—	—
	Dmol [23]	—	2.52	—	—
	Dmol [29]	—	—	2.93	—
	Dmol [33]	—	—	—	3.16
	Pauling [41]	2.20	2.42	2.82	3.12
Experiment	XSW [33]	—	—	—	2.94 ± 0.06
	XSW [27]	—	—	2.81 ± 0.09	—
	XSW [10]	—	2.58 ± 0.04	—	—
	XRD [11]	—	2.55 ± 0.01	—	—
	SEXAFS [12]	—	—	2.88 ± 0.03	—
	Ion channelling [28]	—	—	2.8 ± 0.1	—

3. Results

3.1. Geometry

Fully relaxed atomic geometries have been obtained for all four systems considered and are shown in figure 2. The overlayer dimers were found to be symmetric in all cases, but there are subtle changes in surface relaxation in going from the P overlayer through to the Bi overlayer. Dimer bond lengths are presented in table 1, alongside lengths either predicted in other calculations or measured by experiment, on the whole showing good agreement.

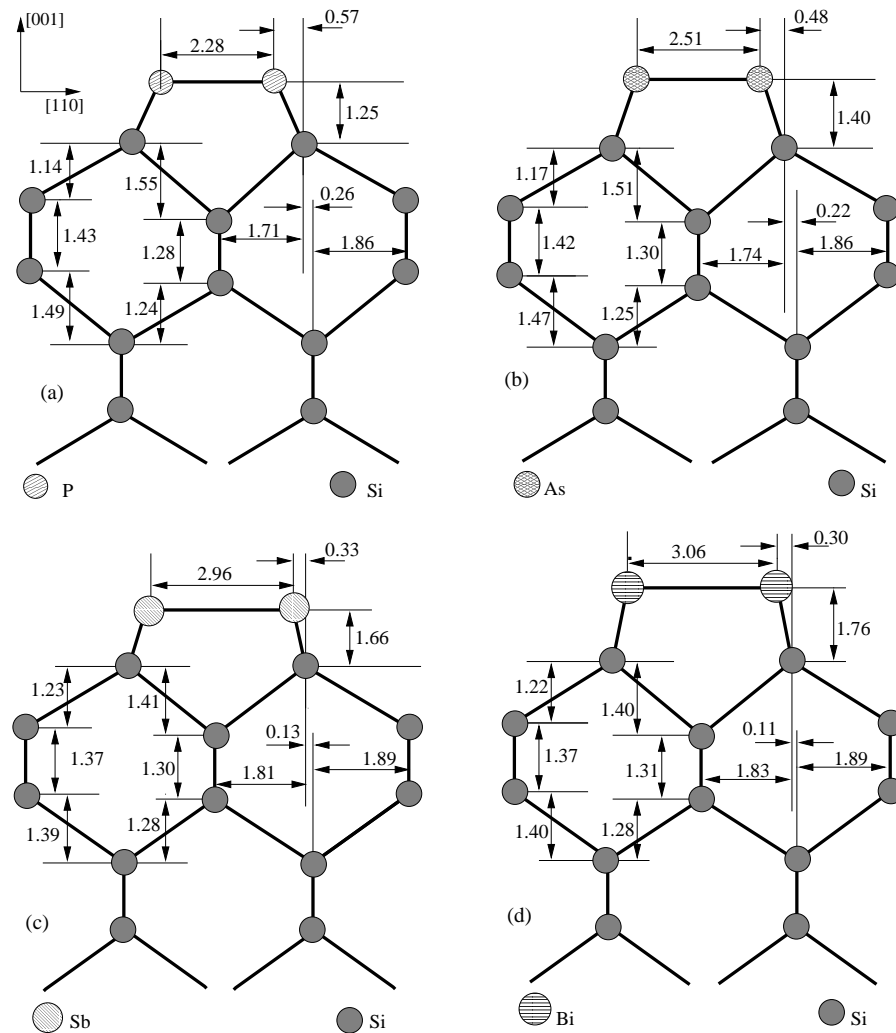


Figure 2. Calculated relaxed geometries for the four Si(001)/V-(2×1) reconstructed surfaces: (a) P overlayer; (b) As overlayer; (c) Sb overlayer; (d) Bi overlayer. The units are Å.

Back-bond lengths and dimer heights above the substrate are shown in tables 2 and 3. Where available, experimental results have been included for comparison. It should be noted, however, that whilst the dimer height above the substrate is easily accessible to theory, the XSW measurements quoted refer to the height of the dimer above the extrapolated bulk-like position of the top substrate layer. Clearly the vertical displacement of the top substrate layer has the vital role in linking these two different definitions of dimer height, but the absolute values of vertical displacements in theoretical calculations are dependent upon how many layers are allowed to relax. We have tried to minimize such interpretational difficulties by clearly labelling theoretical dimer heights and XSW dimer heights as distinct entities in our table, and by including figures for the vertical displacement of the top substrate layer.

As already noted, all four systems share essentially the same basic relaxation mechanism, as shown in figure 3, with only minor discrepancies. The mechanism essentially involves

Table 2. Back-bond lengths (in Å) for (2×1) group V overlayers on Si(001). The Pauling radius for back-bonds is taken as the tetrahedral covalent radius.

		P	As	Sb	Bi
Theory	LDA (this work)	2.35	2.42	2.56	2.62
	LDA [31]	—	—	2.55	—
	LDA [26]	—	2.45	2.59	—
	LDA [30]	—	—	2.58	—
	LDA [25]	—	2.44	—	—
	LDA [24]	—	2.42	—	—
	Dmol [23]	—	2.45	—	—
	Dmol [29]	—	—	2.61	—
	Dmol [33]	—	—	—	2.68
	Pauling [41]	2.27	2.35	2.53	2.63

Table 3. Dimer heights above the substrate (h) and upward shifts (Δz) of top-layer Si atoms (in Å) for (2×1) group V overlayers on Si(001). Also tabulated is $h' = h + \Delta z$, the dimer height measured in XSW.

			P	As	Sb	Bi
Theory	h	LDA (this work)	1.25	1.40	1.66	1.76
		LDA [30]	—	—	1.70	—
		Dmol [23]	—	1.43	—	—
		Dmol [29]	—	—	1.73	—
		Experiment	h	SEXAFS [12]	—	—
Theory	Δz	LDA (this work)	0.04	0.01	-0.10	-0.06
		LDA [31]	—	—	0.05	—
		LDA [26]	—	-0.08	0.03	—
		LDA [25]	—	-0.09	—	—
		Dmol [33]	—	-0.03	—	-0.05
		Dmol [27]	—	—	-0.05	—
Experiment	Δz	XSW, SEXAFS [27]	—	—	-0.10 ± 0.07	—
		Ion channelling [28]	—	—	-0.09 ± 0.07	—
Theory	h'	LDA (this work)	1.29	1.41	1.56	1.70
		LDA [10]	—	1.40	—	—
		Dmol [33]	—	—	—	1.80
Experiment	h'	XSW [33]	—	—	—	1.73 ± 0.01
		XSW [27]	—	—	1.64 ± 0.02	—
		XSW [10]	—	1.40 ± 0.01	—	—
		Ion channelling [28]	—	—	1.63 ± 0.07	—

top-layer Si atoms (3 and 4 in figure 3) being pulled towards each other, as a consequence of the overlayer dimerization (atoms 1 and 2). This movement in turn distorts the rest of the substrate layers beneath, depressing the Si atoms situated directly below the dimer row (6 and 8), and raising those situated outside the line of the dimer row (5 and 7). Table 4 shows the size of the shifts from the ideal positions, with negative entries indicating the limited number of rather small movements in opposite directions to those depicted in figure 3.

Within this generic picture, certain chemical trends are apparent. As expected, the dimer bond and back-bond lengths increase more or less in line with the Pauling radii as we move down the group V column. There is, however, a tendency for the Pauling radii to suggest

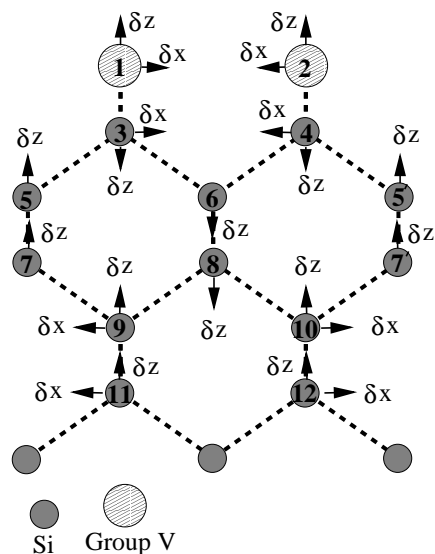


Figure 3. A diagram showing the general relaxation mechanism for the four overlayer systems.

Table 4. A table showing the size of the shifts in Å away from the Si bulk positions. The directions are defined by figure 3.

Element	Atom	Component	P	As	Sb	Bi
Adatom	1	δ_x	0.78	0.66	0.45	0.38
		δ_z	-0.06	0.05	0.20	0.35
	2	δ_x	0.78	0.66	0.44	0.39
		δ_z	-0.06	0.05	0.20	0.35
Si	3	δ_x	0.21	0.18	0.10	0.09
		δ_z	-0.04	-0.01	0.10	0.06
	4	δ_x	0.21	0.18	0.10	0.09
		δ_z	-0.04	-0.01	0.10	0.06
	5	δ_z	0.25	0.20	0.00	0.08
	6	δ_z	0.15	0.15	0.16	0.10
	7	δ_z	0.18	0.13	0.01	0.06
	8	δ_z	0.09	0.09	0.11	0.05
	9	δ_x	0.05	0.05	0.02	0.02
		δ_z	0.04	0.01	-0.03	0.02
	10	δ_x	0.05	0.05	0.02	0.02
		δ_z	0.04	0.01	-0.03	0.02

slightly short adatom-related bonds for overlayers towards the top of the periodic table and slightly long adatom-related bonds towards the bottom.

Interestingly, all Si-Si bonds situated directly beneath the dimer row (bonds C, E and G in figure 1) have similar lengths, at around 2.31 Å, regardless of the adsorbate species. The different substrate relaxations for different adsorbates are thus primarily accommodated by changes in the Si-Si bonds situated outside the line of the dimer row (bonds D, F and H in figure 1). Table 4 reveals that the distortions in the substrate are greatest for the P overlayer, decreasing as one moves down the periodic table towards Sb and remaining much the same from Sb to Bi.

We find P to have the shortest dimer length at 2.28 Å, bonded very close to the Si surface

at a distance of 1.25 Å. The P–Si back-bond has a length of 2.35 Å, in fairly good agreement with the sum of the tetrahedral covalent radii of Si and P. Top-layer substrate atoms 3 and 4 are pulled substantially towards each other by the overlying dimer, each being displaced laterally by 0.21 Å from its ideal position. In consequence, there is considerable distortion in the second and third substrate layers, with a vertical separation of 0.40 Å opening up between second-substrate-layer atoms 5 and 6, and of 0.27 Å between third-substrate-layer atoms 7 and 8.

Arsenic has a rather longer dimer bond length than P of 2.51 Å, consistent both with its larger covalent radius and with experiment [10]. This dimer length is also remarkably close to that previously obtained by Tang and Freeman [23] using a first-principles LDA molecular cluster approach and by Krüger and Pollmann [24] using a Gaussian-orbital-basis Green's function scattering theory. Slightly larger values have been calculated by two other groups using a first-principles plane-wave pseudopotential method: Uhrberg *et al* [25] obtained 2.55 Å and Cho and Kang [26] obtained 2.57 Å.

We also find that the dimer has moved considerably away from the substrate (as compared with the height of a Si dimer on the clean surface) to a distance of 1.40 Å, in very good agreement with XSW results [10]. Good agreement with tetrahedral covalent radii is obtained for the As–Si back-bond length at 2.42 Å, and this length is in perfect agreement with that obtained by Krüger and Pollmann [24]. However, unlike Krüger and Pollmann, we find that the Si substrate is again significantly distorted, although less than in the case of P. Top-layer Si atoms are displaced laterally by 0.18 Å towards the dimer centre, with the vertical separation between second-substrate-layer atoms 5 and 6 being 0.34 Å, and that between third-substrate-layer atoms 7 and 8 being 0.22 Å.

The Sb overlayer has a dimer bond length of 2.96 Å which, although not entirely consistent with its covalent radius, does appear very close to other theoretically obtained Sb–Sb bond lengths for this system (see table 1). However, experiments seem to suggest a shorter dimer length, closer to the figure obtained from the tetrahedral covalent radius of Sb. The vertical separation between the substrate and dimer, on the other hand, is calculated to be 1.66 Å, which does agree with XSW [27] and ion-channelling measurements [28]. From surface extended x-ray absorption fine-structure (SEXAFS) measurements, a larger dimer–substrate separation has been obtained, which is in better agreement with the calculations of Tang and Freeman [29] using Dmol and of Yu and Oshiyama [30] using a plane-wave pseudopotential method). Our calculated Sb–Si back-bond length is 2.56 Å; very close to the sum of the appropriate tetrahedral covalent radii and reasonably close to other theoretical values.

The distortion in the Si substrate beneath the Sb overlayer is somewhat reduced in comparison to the P and As overlayer systems. Although the top-layer Si atoms relax both laterally inwards and vertically downwards by 0.10 Å, the induced vertical separation between second-substrate-layer atoms is now only 0.16 Å. Experiments [27, 28] indicate a similar overall downward relaxation of the surface, although the quoted errors are high enough to cast some doubt on the significance or coincidence of this agreement. Other theoretical studies predict a smaller relaxation of the substrate; both Takeuchi [31] using a plane-wave pseudopotential method and Tang and Freeman [29] using Dmol found the top layer to relax inward by 0.05 Å. However, Takeuchi only relaxed the top four Si layers, whereas we relax six. Aside from this discrepancy, our results on the whole agree very well with those of Takeuchi.

We have made convergence tests for some key structural parameters with respect to the slab thickness and the number of relaxed layers. We find that well-converged results can be obtained for a slab containing at least six substrate layers and allowing for at least four

Table 5. A table showing how certain parameters vary with the change in the number of relaxed layers and slab thickness for the Sb overlayer system. Measurements are in Å and definitions as in table 3.

Slab thickness in No of Si layers	8	8	5
No of relaxed layers	5	3	3
h	1.66	1.67	1.66
Vertical component of C bonds	1.41	1.43	1.43
Vertical component of D bonds	1.23	1.24	1.23
Δz	-0.10	-0.02	-0.03

relaxed substrate layers. The sensitivity of the dimer height to the number of layers allowed to relax is demonstrated in table 5 for the Sb overlayer system. For a slab containing eight Si layers, a change in the relaxation from three to six substrate layers decreases the vertical height of the top substrate layer by more than 0.06 Å. However, inter-layer and inter-atomic distances have not significantly changed. Keeping these observations in mind we can compare our results to those of Cho and Kang [26]: they only allowed three Si layers to relax, and obtained an *outward* relaxation of the top-layer Si atoms of 0.03 Å. Thus while their predictions for the *relative* distortions of the top three substrate layers are in agreement with our own, their calculated *absolute* atomic displacements from the ideal structure are uniformly shifted, due to relaxing fewer layers.

Finally, the dimer length for the Bi overlayer is a little longer than that for Sb at 3.06 Å, in good agreement with the covalent radius for Bi. The length calculated by the Dmol method is considerably greater at 3.16 Å [29], while the XSW technique yields a considerably smaller dimer length of 2.94 ± 0.06 Å [32]. The dimer–substrate separation is now 1.76 Å and is fairly close to XSW experiment [33], while the Bi–Si back-bond has a length close to that of Sb–Si at 2.62 Å, in excellent agreement with the sum of the tetrahedral covalent radii and close to the length calculated by Dmol. The substrate distortion has not greatly changed in going from Sb to Bi, with the vertical separation between neighbouring Si atoms in the second substrate layer increasing slightly to 0.18 Å and the lateral shift of the top-layer Si atoms dropping only by 0.01 Å to 0.09 Å. From a structural point of view the Bi and Sb systems are very similar indeed.

3.2. Bonding

Adsorbate–adsorbate and adsorbate–substrate bonding were studied by examining the total charge density throughout the supercell for the four systems. In each case, the charge density is normalized to the same number of electrons per supercell. Figure 4 shows an oblique slice through each dimer, revealing not only the dimer bonds but also the back-bonds to the substrate. The dimer bond is seen to be strongly covalent in all cases and perfectly symmetric. In fact, the Bi dimer bond shows an interesting double-hump feature, indicating that wavefunction overlap may not be as complete as in the lighter members of the group.

Although the bond strength is determined by far more than simply the peak charge density, considerable insight may be gained by making just such a naive *ansatz*, when comparing similar bonds. On this basis we can compare the strengths of the different V–V dimer bonds, and similarly the strengths of the different V–Si back-bonds. From figure 4 we thus note that the P–P dimer bond is the strongest and the Bi–Bi dimer bond the weakest. Similarly we note that the P–Si back-bond is the strongest and the Bi–Si back-bond the weakest. These bond strength trends for the V–V dimers and the V–Si back-bonds are

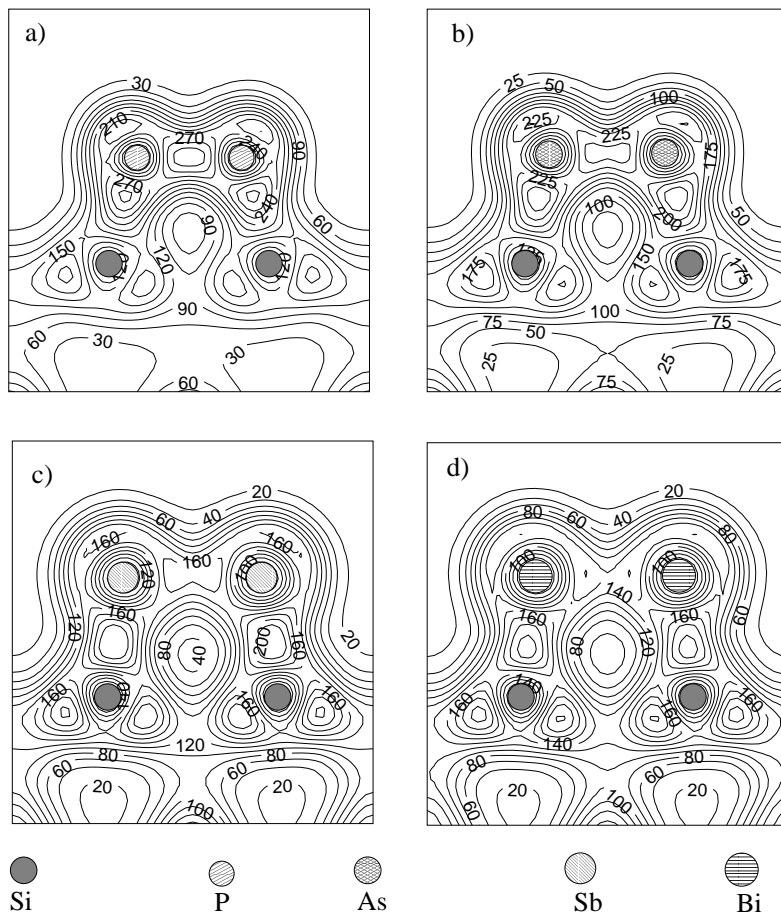


Figure 4. Total charge-density plots for oblique slices through the adsorbate dimer and top-layer Si atoms, showing the nature of the dimer back-bonds in the case of (a) P, (b) As, (c) Sb and (d) Bi overlayers. The contours are normalized to 78 electrons per supercell volume of 16.26 Å³.

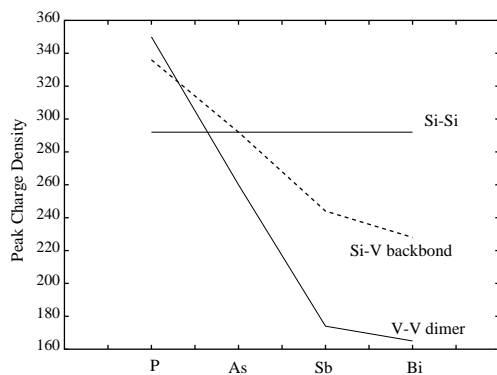


Figure 5. A graph showing the trends in peak charge densities for the V-V dimer bonds and Si-V back-bonds. The Si-Si values are also shown. The values are normalized as explained in figure 4.

summarized in figure 5.

In the cases of P and As, the plots reveal a small charge transfer from the substrate to the dimer, evident from slight displacements of the back-bond charge-density maxima from the

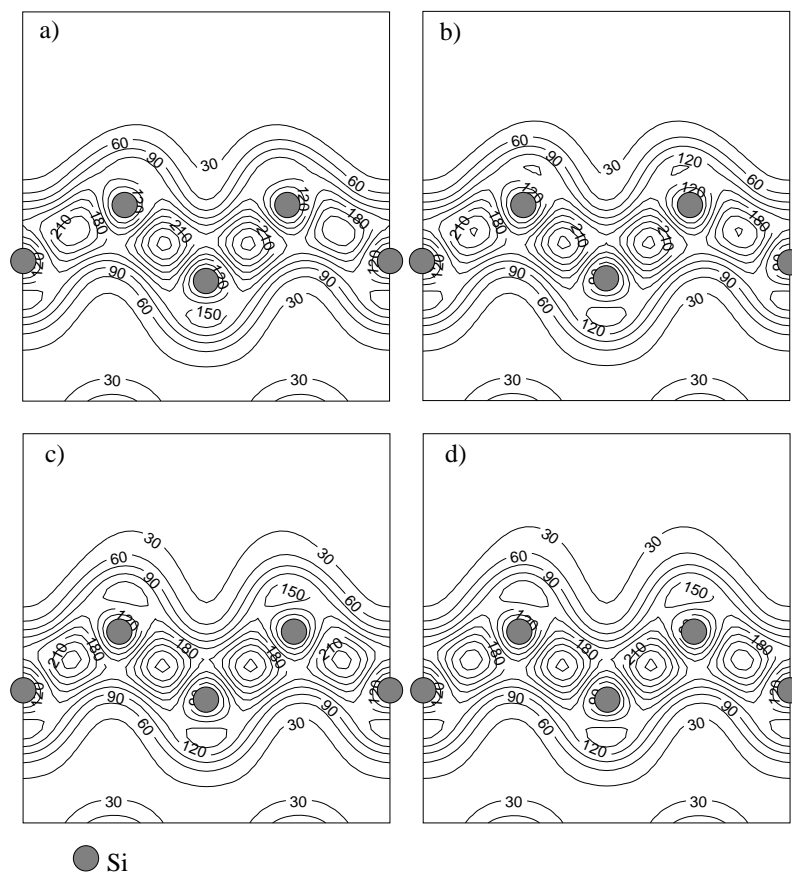


Figure 6. Total charge-density plots for vertical slices through the two topmost Si substrate layers in the case of (a) P, (b) As, (c) Sb and (d) Bi overlayers. The contours are normalized as explained in figure 4.

bond centre. This charge transfer has been observed experimentally by Cole *et al* [34] in the case of As, who estimated a transfer of 0.05 electrons per atom using Auger spectroscopy. If anything, the charge transfer for P is more pronounced. In contrast, although we also see some charge transfer from the dimer to the substrate for the Sb and Bi overlayer systems, the effect is tiny, and so we concur with Koval *et al* [35] that in the case of Bi the bonding for this system is almost purely covalent.

The observed transfer can be correlated to the electronegativity difference between the adsorbate and the substrate. Various electronegativity scales exist, but the general trend is that as one moves down the group V column of the periodic table the electronegativity decreases, due to increased screening of the core by filled electron shells. The Pauling electronegativities for Si, P, As, Sb and Bi are 1.90, 2.19, 2.18, 2.05 and 2.02 respectively. While the adsorbate–overlayer electronegativity difference is large for P and As, it is much smaller for Sb and Bi. It should be emphasized that electronegativities may only be used as a guide and that the ability of an atom to attract electrons depends greatly on its chemical environment.

Figure 6 is a vertical slice through the two top Si substrate layers. Although these plots only slice through Si atoms, charge associated with the Si–overlayer bond may be seen

Table 6. Si–Si bond lengths (in Å) in the top four substrate layers for (2×1) group V overlayers on Si(001). See figure 1 for the labelling of the bonds. The bulk Si–Si bond has a theoretical length of 2.35 Å.

Bonds	P	As	Sb	Bi
C	2.30	2.31	2.30	2.30
E	2.31	2.31	2.32	2.32
G	2.33	2.33	2.32	2.32
D	2.42	2.40	2.36	2.35
F	2.39	2.39	2.36	2.36
H	2.39	2.38	2.35	2.36

above the uppermost pair. In the case of Sb and Bi, this charge is considerable, reflecting the covalent nature of the bonds. In the case of P and As, where some charge transfer has taken place from these Si atoms to the dimer (and, therefore, a smaller component of the back-bond is in this plane), considerably less charge is seen to localize itself around these atoms. Despite different degrees of distortion in the top substrate layer, all of the Si–Si bonds marked ‘C’ in figure 1 have the same peak density. However, the bonds marked ‘D’ in figure 1 do change in terms of peak charge density over a small range, in the ratio 267:272:282:287 for the P, As, Sb and Bi overlayers respectively, although this is not apparent in figure 6, due to our selection of a convenient contour spacing. This increase in peak charge density is consistent with the shortening in length of these bonds as one goes from a P to a Bi overlayer (see table 6).

3.3. Band structure

The electronic band structures of the four overlayer systems were calculated and are shown in figure 7. All four show very similar dispersions, as one might expect; each has three surface bands inside the bulk semiconducting gap. Nevertheless, all of these adsorbates possess a passivating property, as the fundamental band gap of Si is cleared of the surface states present on the clean surface. One of these states is unoccupied and is found close to the conduction band edge for a part of the Brillouin zone and appears to be $pp\sigma^*$ related. The other two are occupied π -like surface states just below the valence band maximum, identified as an *ungerade*-like bonding state (π_u) and a *gerade*-like antibonding state (π_g). As described in previous work [15], these states are very similar to those seen for the symmetric C=C dimer on the diamond (001) surface [36], except that in that case the antibonding orbital is unoccupied and lies clearly above the bonding energy state. In the case of group V adsorbates, the extra electron per dimer atom means that the previously unoccupied π_g antibonding state is now fully occupied and that its energy level is substantially dropped down.

The drop in energy of antibonding bands upon finite occupation is well known in semiconductors as the band-gap-narrowing effect (see, for example, the many-body theoretical work of Oschlies *et al* [37]). The effect is due to the presence of intraband exchange interactions not present in the infinitesimal occupancy case. This allows predictions of certain band energies to be made that are based upon isomorphic bands in other systems. In this case, the π_g -orbitals for V–V dimers and C=C dimers look very similar, and the main difference is thus a lowering of the orbital energy for the V–V dimers, relative to C=C, due to additional intraband exchange. The energy of the π_g -state can now be

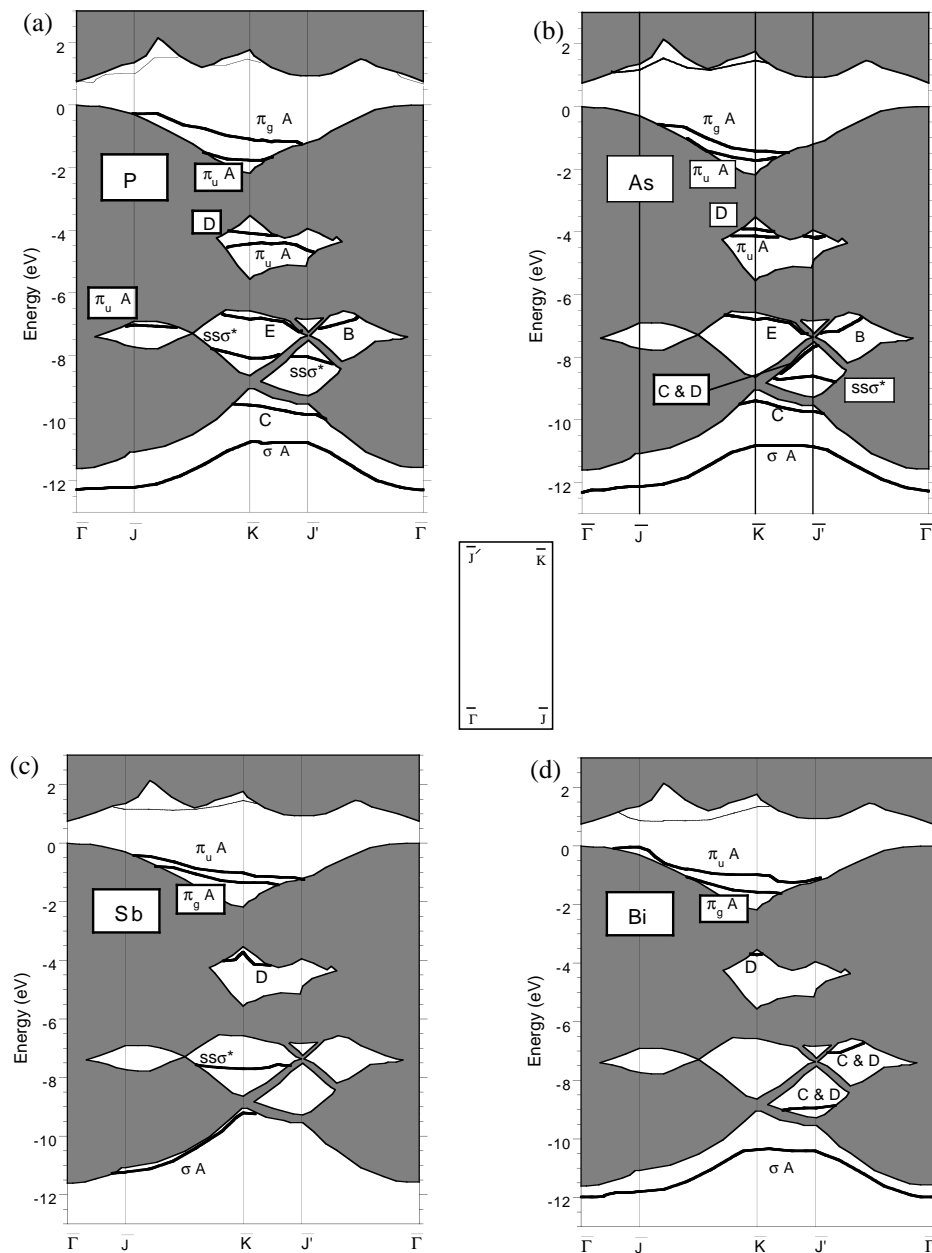


Figure 7. Calculated surface band structures for the four Si(001)/V-(2×1) reconstructed surfaces with (a) P, (b) As, (c) Sb and (d) Bi overlayers. The hatched area denotes the projected bulk band structure of Si, and the inset shows the irreducible segment of the surface Brillouin zone. Surface-state localization is indicated with the bond notation introduced in figure 1.

comparable to that of the π_u -state. The relative positioning of the π_u and the π_g for the various overlayers is shown in figure 8. For Sb and Bi it actually drops below the energy of the π_u -bonding state! Uhrberg *et al* [25] have suggested that the splitting between the π_u - and the π_g -state for the As overlayer depends on the As-As dimer bond length. In their

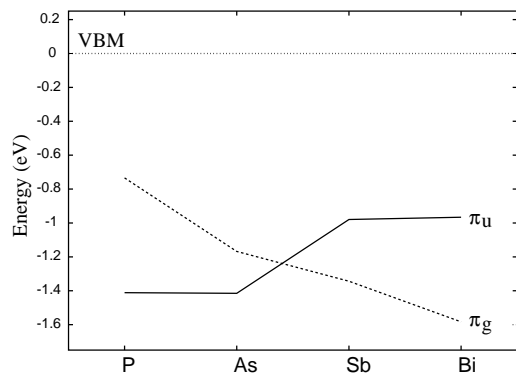


Figure 8. A graph showing the energetic positions of the π_u - and the π_g -states at the \bar{K} point for the different adsorbates.

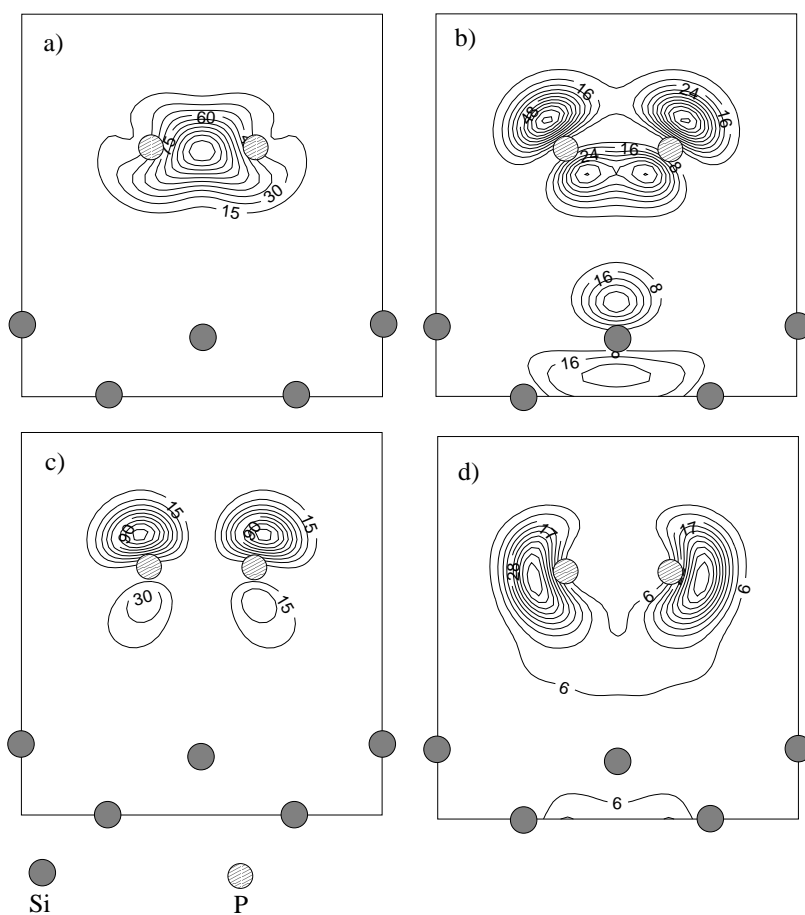


Figure 9. Partial charge-density plots at the \bar{K} point for the P overlayer case in the vertical plane through the dimer for (a) the occupied σ -like state, (b) the occupied π_u -bonding state, (c) the occupied π_g -antibonding state and (d) the lowest unoccupied surface state. The charge density is normalized to two electrons per supercell of volume 16.26 \AA^3 .

LDA calculations they found that the splitting increased as they reduced the length of the As–As dimer. From figure 8 we observe that the splitting has one sign for P and As and

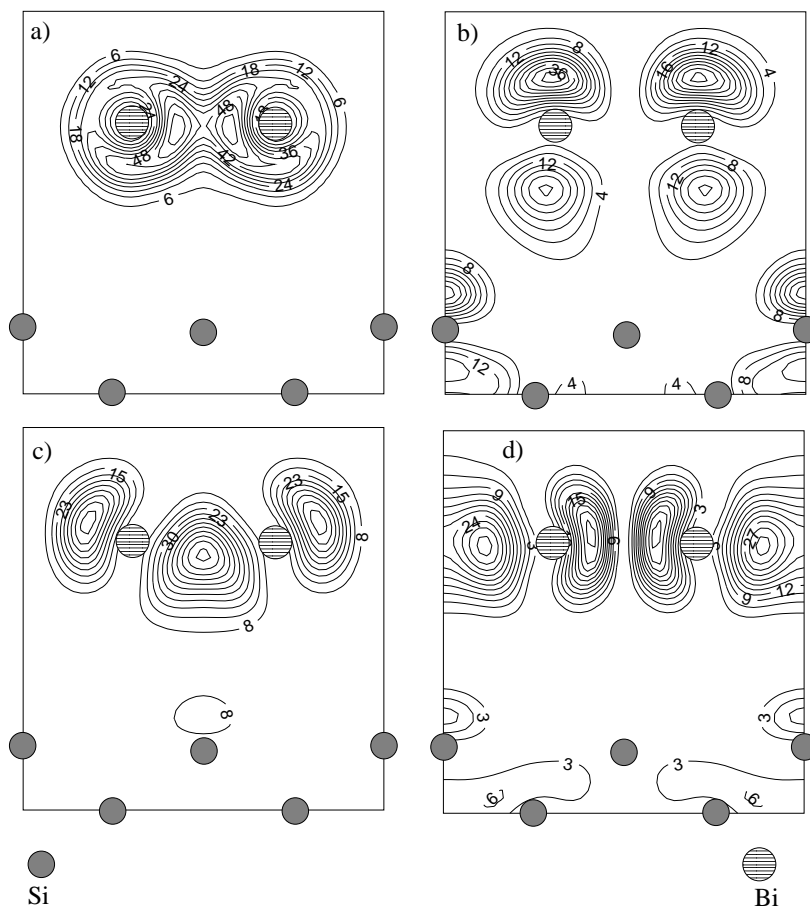


Figure 10. Partial charge-density plots at the \bar{K} point for the Bi overlayer case in the vertical plane through the dimer for (a) the occupied σ -like state, (b) the occupied π_g -antibonding state, (c) the occupied π_u -bonding state and (d) the lowest unoccupied surface state. The normalization is as explained in figure 9.

another for Sb and Bi overlayers. We see that the π_u -band increases in energy as we go from a P to a Bi overlayer whereas the π_g -state decreases in energy. The maximum separation in energy between the π_g - and the π_u -band is ≈ 0.75 eV for the P dimer, ≈ 0.30 eV for the As dimer, ≈ -0.40 eV for the Sb dimer and ≈ -0.60 eV for the Bi dimer. The splitting for the As dimer is similar to that noted by Uhrberg *et al* [25] in their LDA calculations, but they were unable to resolve such a small separation in their angle-resolved photoemission analysis. Partial charge-density plots relating to these states are shown in figure 9 for P and figure 10 for Bi. The corresponding partial charge-density plots for As and Sb were found to be very similar to those for P and Bi respectively.

The four systems all have an $ss\sigma$ -like dimer-related band at the low energy end of the bulk valence continuum (figure 7). The partial charge-density plots relating to these may be seen in figures 9 and 10 (in which the plots for P and Bi may again be taken as also representative of As and Sb respectively). This $ss\sigma$ band lies below the bulk valence bands across the entire surface Brillouin zone for the P, As and Bi overlayers. In the case of Sb, however, the band lies substantially higher in energy, almost entirely in resonance with the

lower edge of the bulk continuum. A similar trend was observed for group V overlayers on the (110) surface of III–V materials by Schmidt *et al* [38].

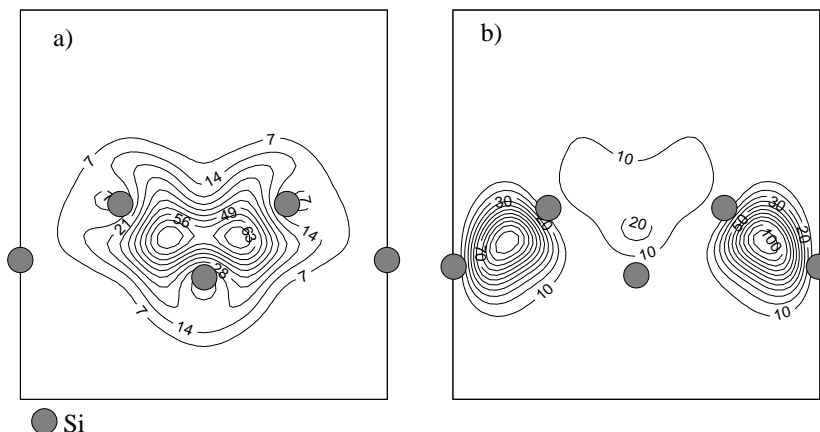


Figure 11. Partial charge-density plots for (a) the As-covered Si(001) surface localized around the ‘C’ bonds calculated at the \bar{K} point and (b) the surface state on the Bi-covered Si(001) surface localized around the ‘D’ bonds, calculated at the \bar{K} point. The normalization is as explained in figure 9.

In addition to the dimer-related surface states, there are a number of other states arising due to overlayer-induced distortions of the substrate. The precise positions of these depend upon the level of substrate distortion present in the system, so once again it is natural that the P and As overlayer systems (for which the substrate is heavily distorted) form a pair, as do the much less distorted Sb and Bi overlayer systems. Correspondingly, we find that the P- and As-covered surfaces possess more complicated patterns of substrate-relaxation surface bands than do the Sb and Bi surfaces. For example, both P and As overlayer systems feature a surface state below the bulk continuum which is formed by hybridization of orbitals localized around the ‘C’ bonds of the substrate (figure 11(a)). The bond angle between these bonds is distorted quite far from its bulk value, so the hybrid energy is quite far from the corresponding value in the bulk. Beneath the Sb and Bi overlayers, however, the distortion in this region is much less and this state becomes resonant with the bulk continuum. Similarly, another substrate-relaxation surface state, localized on the ‘E’ bonds, is also present in the case of the P and As overlayers, but becomes resonant for the Sb and Bi overlayers.

An $ss\sigma^*$ state with various degrees of back-bond characteristic may be seen for the P-, As- and Sb-covered systems (see, for example, figure 12(a)), becoming resonant in the case of a Bi overlayer. A similar state was also described by Krüger and Pollmann [24] in their study of Si(001)/As(2×1). The back-bond component in this state increases as we move down the periodic table from the P to the Sb overlayer. As well as this state, the P- and As-covered systems also possess another state which is even more highly localized on the back-bonds. These states are labelled ‘B’ on the band structures, and the partial charge-density plot for this state in the case of the P overlayer is shown in figure 12(b).

Another notable feature is a surface state localized on the ‘D’ bonds which may be seen at around -4 eV in the upper stomach gap around the \bar{K} point for all four overlayers (see, for example, figure 11(b)). The stability of its energy from one system to another is quite remarkable, considering that the ‘D’ bonds themselves are compressed by around 3% in

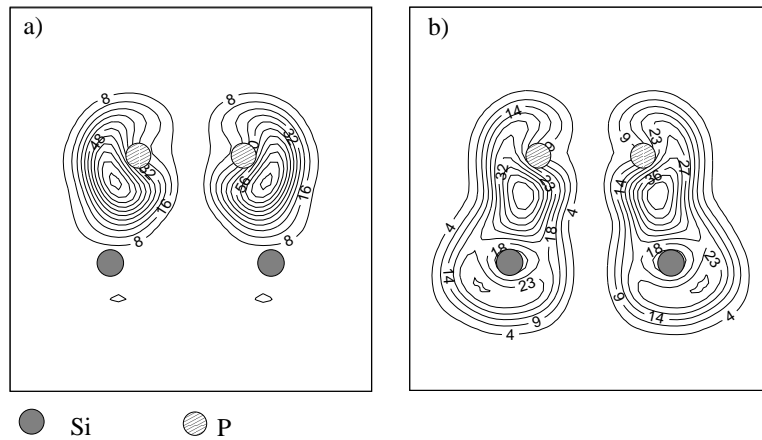


Figure 12. Partial charge-density plots for an oblique slice through dimer and top-layer Si atoms showing (a) partial charge densities for state localized as $ss\sigma^*$ and the back-bond for the P overlayer, calculated at the \bar{K} point and (b) the surface state on the P-covered Si(001) surface localized around the 'B' bonds in the stomach gap along the \bar{J} to $\bar{\Gamma}$ segment. The normalization is as explained in figure 9.

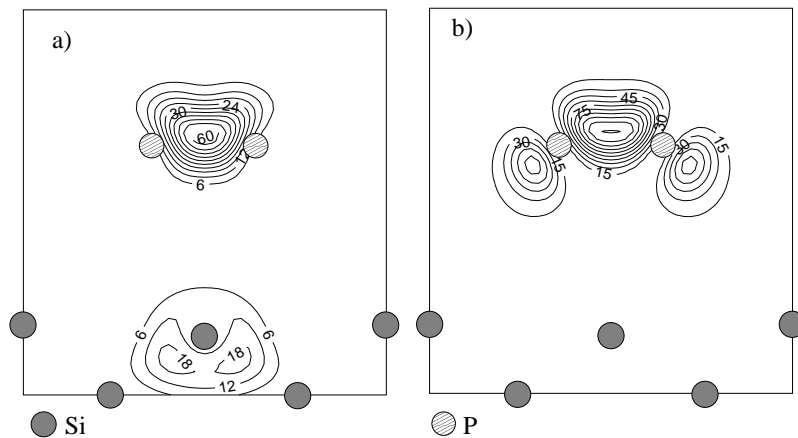


Figure 13. A vertical slice through a dimer showing partial charge-density plots for surface states on the P-covered Si(001) surface (a) in the stomach gap around the \bar{J} point and (b) at a stomach gap around the \bar{K} point. The normalization is as explained in figure 9.

going from P to Bi. In contrast, the 'C' bonds maintain more or less the same length for all four systems, but the states localized on them shift considerably in energy from one system to another, presumably due to changes in the bond angles.

A final point of interest is the appearance of resonant dimer-related bands in the stomach gaps for the P- and As-covered systems. Similar states were seen for the Si(001)/As(1 ML)- (2×1) system by Krüger and Pollmann [24]. The P-covered surface has two such states, one at the \bar{J} point and the other around the \bar{K} point, while the As-covered surface possesses only the state at the \bar{K} point. The state at \bar{J} is almost entirely localized on the dimer and is quite σ -like in appearance (see figure 13(a)). The state at \bar{K} is reminiscent of a π_u -dimer bond, but also has a significant back-bond component (see figure 13(b)).

3.4. Comparison with the clean and monohydride Si(001) surfaces

It is interesting to compare the group V adsorbates on Si(001) with other systems characterized by symmetric dimers. For example, as mentioned in the introduction, the clean Si(001) surface consists of tilted (or buckled) dimers, but if the dimer is artificially constrained to remain symmetric one obtains a system geometrically rather similar to the overlayer cases already discussed. The main difference is that the dimer atoms have only a valency of four, and there are correspondingly two less electrons to occupy the dimer π -orbitals. This results in a semi-metallic situation with a small but finite occupancy of the antibonding π_g -orbital and not-quite-complete occupancy of the bonding π_u -orbital (Krüger and Pollmann [36] describe this situation as metallic, but the band structure that they present actually indicates semi-metallicity, as does our own calculation). In a previous paper such a Si=Si dimer was found to have a length of 2.20 Å [39], substantially shorter than our calculated bulk Si–Si bond length of 2.35 Å, because the σ -plus- π_u combination essentially amounts to a double bond. Twice the covalent double-bond radius for Si is 2.14 Å, in good agreement with the length obtained for the symmetric dimer.

In contrast to this somewhat artificial system, realistic symmetric Si dimers can be obtained by bonding a single hydrogen atom onto each Si atom of the dimer (thus ‘soaking up’ the two electrons shared between the two π -states). The dimer bond length on the resulting ‘monohydride’ Si(001) surface is increased to 2.40 Å [40]. This is in good agreement with twice the covalent single-bond radius of Si which is 2.34 Å. Unlike the semi-metallic symmetric Si=Si dimer, the monohydride structure is semiconducting, with no surface states appearing in the band-gap region at all [40]. The unsaturated π -states have instead dropped in energy upon becoming fully occupied, ultimately re-hybridizing as strongly resonant states associated with the Si–H bonds. The contribution of these states on the dimer bond itself therefore becomes minimal, in a similar manner to the cancellation of occupied π -bonding and antibonding orbitals on group V dimers.

If one considers also the asymmetric tilted Si–Si dimer which has a calculated bond length of 2.25 Å, a clear trend is seen to develop. At one extreme we have the symmetric Si–Si dimer with an almost fully occupied π_u -state resulting in what is essentially a double bond. At the other extreme we have the monohydride situation where electrons of the π_u -state are drawn away by the hydrogen atoms leaving only a σ -like contribution to the dimer, resulting in a much longer single bond. Somewhere between the two is the tilted dimer, where the somewhat distorted π_u -state is still fully occupied. However, as this state has a large component associated with a single-dimer atom, its contribution to the dimer bond is reduced and the dimer bond length is slightly elongated with respect to the symmetric dimer length. With their fully occupied bonding and antibonding π -states largely cancelling out, the group V dimers discussed in this paper show greatest similarity to the monohydride system: only the σ -bond influences the dimer bond lengths, which are consequently in good agreement with the covalent single-bond radii.

4. Conclusions

We have presented fully relaxed geometries for P, As, Sb and Bi adsorbates in the (2×1) reconstruction on the Si(001) surface, identifying a generic relaxation mechanism and detailing chemical trends down the group. Most importantly, the overlayer-induced distortion of the substrate is found to decrease with increasing overlayer atomic number.

All four systems show broadly similar electronic structures and bonding, notably in being semiconducting with the Si fundamental gap free of surface states. In more detail,

we have found that the P and As overlayer systems form a natural pair as regards their electronic and bonding properties, as do the Sb and Bi overlayer systems.

Acknowledgments

SCAG and SJJ are grateful to the EPSRC for financial support. The computational work was supported by the EPSRC (UK) through the CSI scheme.

References

- [1] Lander J and Morrison J 1962 *J. Chem. Phys.* **37** 729
- [2] Cardillo M J and Becker G E 1978 *Phys. Rev. B* **21** 1497
- [3] Wolkow R A 1992 *Phys. Rev. Lett.* **68** 2636
- [4] Inoue K, Morikawa Y, Terakura K and Nakayama M 1994 *Phys. Rev. B* **49** 14 774
- [5] Dabrowski J and Scheffler M 1992 *Appl. Surf. Sci.* **56** 15
- [6] Copel M, Reuter M C, Kaxiras E and Tromp R M 1989 *Phys. Rev. Lett.* **63** 632
- [7] Copel M, Reuter M C, Horn von Hoegen M and Tromp R M 1990 *Phys. Rev. B* **42** 11 682
- [8] Katayama M, Nakayama T, Aono M and McConville C F 1996 *Phys. Rev. B* **54** 8600
- [9] Bringans R D, Uhrberg R I G, Olmstead M A and Bachrach R Z 1986 *Phys. Rev. B* **34** 7447
- [10] Franklin G E, Fontes E, Qian Y, Bedzyk M J, Golovchenko J A and Patel J R 1994 *Phys. Rev. B* **50** 7483 and references therein
- [11] Jedrecy N, Sauvage-Simkin M, Pinchaux R, Massies J and Greiser N 1990 *Surf. Sci.* **230** 197
- [12] Richter M, Woicik J C, Nogiami J, Pianetta P, Miyano K E, Baski A A, Kendelewicz T, Bouldin C E, Spicer W E, Quate C F and Lindau I 1990 *Phys. Rev. Lett.* **65** 3417
- [13] Hanada T and Kawai M 1991 *Surf. Sci.* **242** 137
- [14] Gavioli L, Betti M and Mariani C 1997 *Surf. Sci.* **377** 215
- [15] Jenkins S J and Srivastava G P 1996 *Surf. Sci.* **352–354** 411
- [16] Jenkins S J and Srivastava G P 1997 *Phys. Rev. B* **56** 9221
- [17] Gay S C A, Jenkins S J and Srivastava G P 1998 *Surf. Sci.* **402–404** 641
- [18] Hohenberg P and Kohn W 1964 *Phys. Rev.* **136** B864
- [19] Kohn W and Sham L J 1965 *Phys. Rev.* **140** A1133
- [20] Perdew J P and Zunger A 1981 *Phys. Rev. B* **23** 5048
- [21] Bachelet G B, Hamann D R and Schlüter M 1982 *Phys. Rev. B* **26** 4199
- [22] Umerski A and Srivastava G P 1995 *Phys. Rev. B* **51** 2334
- [23] Tang S and Freeman A J 1993 *Phys. Rev. B* **48** 8068
- [24] Krüger P and Pollmann J 1993 *Phys. Rev. B* **47** 1898
- [25] Uhrberg R I G, Bringans R D and Northrup J E 1986 *Phys. Rev. Lett.* **56** 520
- [26] Cho J-H and Kang M-H 1995 *Phys. Rev. B* **51** 5058
- [27] Lyman P F, Qian Y and Bedzyk M J 1995 *Surf. Sci.* **325** L385
- [28] Grant M W, Lyman P F, Hoogenraad J H and Seiberling L E 1992 *Phys. Rev. B* **279** L180
- [29] Tang S and Freeman A J 1993 *Phys. Rev. B* **47** 1460
- [30] Yu B D and Oshiyama A 1994 *Phys. Rev. B* **50** 8942
- [31] Takeuchi N 1997 *Phys. Rev. B* **55** 2417
- [32] If we use the Bi tetrahedral bond length instead of the Bi covalent radius, a dimer length of 2.92 Å is predicted.
- [33] Franklin G E, Tang S, Woicik J C, Bedzyk M J, Freeman A J and Golovchenko J A 1995 *Phys. Rev. B* **52** R5515 and references therein
- [34] Cole R J, Evans J A, Weightman P, Matthew J A D, Woolf D A and Westwood D I 1994 *Phys. Rev. B* **49** 7528
- [35] Koval I F, Melnik P V, Nakhodkin N G, Pyatnitsky M Y and Afanasieva T V 1995 *Surf. Sci.* **333** 585
- [36] Krüger P and Pollmann J 1995 *Phys. Rev. Lett.* **74** 1155
- [37] Oschlies A, Godby R W and Needs R J 1992 *Phys. Rev. B* **45** 13 741
- [38] Schmidt W G, Bechstedt F and Srivastava G P 1996 *Surf. Sci. Rep.* **25** 141
- [39] Tütüncü H M, Jenkins S J and Srivastava G P 1997 *Phys. Rev. B* **56** 4656
- [40] Çakmak M and Srivastava G P 1998 private communication
- [41] Burns G 1985 *Solid State Physics* (Orlando, FL: Academic)